Available online at www.sciencedirect.com

SciVerse ScienceDirect

Advances in Space Research 49 (2012) 1670–1683

ADVANCES IN SPACE RESEARCH (a COSPAR publication)

www.elsevier.com/locate/asr

New ^{3}He neutron monitor for Chilean Cosmic-Ray Observatories from the Altiplanic zone to the Antarctic zone

E.G. Cordaro [a], E. Olivares [b], D. Galvez [a], D. Salazar-Aravena [c], D. Laroze [d,e,*]

[a] *Observatorios de Radiación Cósmica, Universidad de Chile, Casilla 487-3, Santiago, Chile*
[b] *Escuela de Ingeniería Electrónica, Facultad de Ingeniería, Universidad Mayor, Av. Manuel Montt 367, Santiago, Chile*
[c] *Departamento de Física, Universidad de Santiago de Chile, Av. Ecuador 3493, Santiago, Chile*
[d] *Max Planck Institute for Polymer Research, D 55021 Mainz, Germany*
[e] *Instituto de Alta Investigación, Universidad de Tarapacá, Casilla 7D, Arica, Chile*

Received 18 November 2010; received in revised form 7 March 2012; accepted 9 March 2012
Available online 20 March 2012

Abstract

We present the results of three years of continuous operations and the principal characteristics of our new ^{3}He neutron monitors installed in the Chilean Network of Cosmic-Ray Observatories. During the years 2004 and 2005, we began the construction of this International Geophysical Year (IGY)-type ^{3}He neutron monitor, with the intention of replacing the older proportional tubes of the BF_3. These new monitors are installed in stations at locations ranging from the near-equatorial zone to the Antarctic zone. As a reference system, we used our own BF_3 neutron monitors and previously complemented the collected data with a Monte Carlo simulation for the proton-yield function response of the Putre neutron monitor. Herein, we present for the first time the data obtained from our new high-mountain observatory located in the Altiplanic zone.

Keywords: ^{3}He neutron monitor; High mountain observatories; Ground level event; Monte Carlo method

1. Introduction

The Chilean Network of Cosmic-Ray Observatories has four stations that cover almost the entire southern hemisphere. The northernmost station, the "Putre-Incas" High-Mountain Observatory, began operating in November, 2003 and is located in the Altiplanic Andean region over the Tropic of Capricorn zone at the International Center for Andean Studies – Incas; its geographic coordinates are 18.197 S 69.55 W, and its altitude is 3598 [m.a.s.l.]. Additionally, the geomagnetic rigidity is 11.73 [GeV]. The main instruments are a three counter neutron monitor of International Geophysical Year (IGY) type: 3IGYNM and an multidirectional muon telescope: MMU. The 3IGYNM was originally shipped with *BP9D*-BF_3 proportional neutron counters, and since August 2007, it has been equipped with *LND25384*-^{3}He proportional neutron counters.

The Antarctic Cosmic-Ray Observatory (Laboratorio Antártico Radiación Cósmica; LARC) was built in 1991. It is located at Fildes Bay, on King George Island, one of the South Shetland Islands, at geographic coordinates 62.20 S 58.96 W and an altitude of 40 [m.a.s.l.]; it has a geomagnetic rigidity of 2.71 [GeV]. This observatory is equipped with a standard *IQSY 6NM64* neutron monitor and *BP-28* BF_3 proportional neutron counters. This type of instrumentation is used around the world for the continuous measurement of cosmic rays reaching the terrestrial environment. In 2007, the 3NM64-^{3}He neutron monitor, built by the Italian Cosmic-Ray Group in Rome, arrived at the LARC. In collaboration with the Italian Group, we re-assembled the monitor and made it operational on

* Corresponding author at: Max Planck Institute for Polymer Research, D 55021 Mainz, Germany. Tel.: +49 (0)6131 379165; fax: +49 (0)6131 379340.
E-mail address: laroze@mpip-mainz.mpg.de (D. Laroze).

0273-1177/$36.00 © 2012 COSPAR. Published by Elsevier Ltd. All rights reserved.
http://dx.doi.org/10.1016/j.asr.2012.03.015

site. A new 3NM64-^{3}He neutron monitor, built integrally in Chile, was added to the LARC in late 2007. This work was performed from 1995 to 2011 in an existing collaboration between Chile and Italy (UChile/IFSI-INAF/Uni-RomaTre/PNRA Italy /INAch logistic) (Storini and Cordaro, 1997; Cordaro and Storini, 2001).

The Los Cerrillos Observatory for Cosmic Rays (Observatorio Los Cerrillos; OLC), constructed in 1948, is located in *Santiago de Chile*. Its geographic coordinates are 33.50 S 70.72 W. The observatory possesses a geomagnetic rigidity of 9.53 [GeV]. During the first years of the 1980s, the Multidirectional Muon Telescope, with eight photo-multipliers and seven channels of data, was built and made fully operational. Between 1989 and 1990, a 6NM64 neutron monitor with BP28-BF_3 proportional counters was reconstructed, modernized and put into operation. This neutron monitor was transported to the Antarctic territory in 1991 (at the E. Frei Base of the Chilean Air Force on King George Island). In 2001, a 6NM64 neutron monitor, with the same configuration as the LARC Antarctic 6NM64 neutron monitor, was built at the OLC. This instrument and the OLC Observatory are together called a "mirror" of the LARC Observatory because the temporal and spatial coincidences of the same events are registered, and the instrumental configurations are very similar.

The O'Higgins Observatory (OHI) was constructed in 2004 at the O'Higgins Chilean Army Antarctic Base. Its geographic coordinates are 63.32 S 57.9 W, and its geomagnetic rigidity is 2.70 [GeV]. This observatory is equipped with a UCLA-IGPP fluxgate magnetometer, and the installation of a new NM-^{3}He is under study.

All the stations of the Cosmic-Ray Observatories feature a UCLA-IGPP fluxgate magnetometer, installed as part of a collaboration with the SAMBA-UCLA-USA project. This type of magnetometer measures and records three geomagnetic components and environmental values.

1.1. About the neutron monitors

The neutron monitor (NM) is the standard instrument used to detect the nucleonic component of cosmic rays. The first neutron monitor of the IGY type was built by Simpson in 1948. The monitor pile structure remained the same until a large BP-28 counter was introduced in 1959 at Chalk River Laboratories. The next step was the creation of the first 6NM64 neutron monitor design. The number before the initial letter indicates the number of proportional counters in the array.

Neutron monitors are composed of four principal parts: reflector, producer, multiplier and counter. The producer surrounding the counter is generally made of lead, which is shaped into a ring or a brick, because lead is an element with a high nucleonic density that produces a high yield of neutrons in inelastic reactions, providing an approximately eightfold increase.

The classic equation ${}_5B^{10} + {}_0n^1 \rightarrow ({}_3Li^7 + 0.9\,\text{MeV}) + ({}_2He^4 + 1.6\,\text{MeV})$ explains the reaction occurring in a proportional counter when a slow neutron collides with an isotope B^{10}, generating a resonant exothermic nuclear reaction inside of a proportional counter filled with BF_3 enriched with B^{10}. As a result of this reaction, an energy of 2.5 [MeV] is liberated, 1.6 [MeV] corresponding to alpha particles and 0.9 [MeV] to the ${}_3Li^7$ nucleus. The two particles travel in opposite directions in a gas and generate approximately 80,000 ion pairs for a fully utilized mean free path (Vekler et al., 1950). For this reason, the operation of the neutron counter is stable at an amplification factor of several thousand.

Similarly, in a modern proportional neutron counter filled with ^{3}He, the response neutrons for the exothermic reaction of ^{3}He (n,p) ^{3}H liberate an energy of 765 [keV]. Another important point is the production of natural boron, which consists of two isotopes, approximately 20% ${}_5B^{10}$ and 80% ${}_5B^{11}$, but only ${}_5B^{10}$ participates in the reaction, liberating an energy of approximately 480 [keV]. Because the counting effectiveness is determined by the probability of neutron capture by boron nuclei and the capture cross-section for a range of neutron energies reaches its maximum value for thermal neutrons, in this configuration, the counter primarily records thermal neutrons. The general properties of ^{3}He proportional counters and their related effects were surveyed by Mills et al. (1962). In general, neutrons deposit their energy as ions, producing electrical pulses called neutron-produced pulses, which can be selected by a pulse-height discriminator. An increase in the high voltage beyond the ionization plateau can produce what is called an avalanche process, wherein the gas amplification is proportional to the primary ionization; for this reason, a high-gain amplifier is required.

The moderator in the IQSY design is usually a thin-walled cylinder (with a thickness of 2 [cm]) made of polyethylene that surrounds the proportional counter and separates it from the lead producer. The moderator reduces the energy of the generated neutrons to the thermal level. This moderation increases the probability of neutron capture by the gas inside the proportional counter.

The first reflector model was made of solid paraffin. However, modern reflectors are made of layers of polyethylene bricks that surround the producer and the proportional counters. Their purpose is to maintain low-energy neutrons inside the detector and to create a shield against local external radiation.

2. Materials and methods

2.1. The old and new neutron counters

Both the measurement instruments and their proper calibration are critical to the operation of neutron monitors; these problems that must be addressed before replacing proportional counters.

At both stations, the Putre-Incas High-Mountain Observatory and the LARC Antarctic Observatory, the cost of building a proportional counter of the BF_3 type is very

high, and the design process is lengthy. Thus, we must research alternatives to obtain continuous measurements in remote zones. One alternative for obtaining cosmic-ray measurements is to exchange the old proportional neutron counters BP9-D and BP28 for the ^{3}He LND25384 and LND25373 proportional neutron counters.

The purpose of this exchange is to obtain a new proportional counter with a better range of detection of particles associated with galactic and solar cosmic rays. We conducted a comparative test involving simultaneous measurements with both types of neutron monitors with proportional counters: the BP9-D and LND; moreover, we conducted a comparative test between the two types of LND counters.

We tested and analyzed the LND25384 and LND25373 ^{3}He proportional counter types and their new design as high-gain amplifiers and pulse-height discriminators, which are the critical instrumental components for neutron monitoring operations. This new type of proportional counter replaced the BP9-D counter and the 3IGYNM-BF_3 systems in the Altiplanic zone, and a new 3NM64 section was added to the 6NM64-BF_3 neutron monitor in Antarctica.

In this case, detector calibration must be performed by comparing the results of measurements with cosmic-ray different arrays combined with detectors equipped with either BF_3 or ^{3}He at a single observation point under identical conditions. Data acquisition is performed by independent electronic circuits in these systems, making it possible to compare results, control the operation of the installations and increase the reliability of the collected data.

2.2. Geometry of the neutron monitor

We maintained the geometries of both neutron detectors in the comparative test of proportional counters because prior studies have shown that approximately 84% of the recorded neutrons are formed in the lead producer, 13% are formed in the paraffin or polyethylene, and only 3% correspond to background radiation from the counter or neutrons that arrive at the detector from the outside (Simpson et al., 1953).

The reflector used in the BF_3 and ^{3}He neutron monitor is composed of low-density polyethylene, a component with a total length of 222 [cm], a total diameter of 315 [cm] and a total depth of 52 [cm], with a thickness of 7.5 [cm] and an average thickness of 7.0 [cm]. The moderator material used is low-density polyethylene; the moderator is cylindrical in shape, with a thickness of 2.0 [cm] and a diameter of 24.5 [cm].

In the IGY neutron monitor, the reflector is composed of paraffin wax bricks and aluminum. Its total length is 114.3 [cm], its total width is 111.76 [cm], and its total height is 58.42 [cm], with a thickness of 10.9 [cm] and an average thickness of 11.0 [cm]. The moderator material used is paraffin wax. The thickness of the moderator, which is rectangular in shape, is 15.3 [cm].

2.3. The high-gain amplifier and pulse-height discriminator for a new type of ^{3}He neutron monitor

The aim of the first test conducted was to determine the output pulse activity of the BF_3 proportional counter. This unit is polarized using only high voltage, and the output signal is amplified using the standard Chalk River module.

The pulse amplitude spectrum of the BF_3 counter shows peaks at 2.30 [MeV] and 2.70 [Mev] due to the two forms of neutron capture. The ideal pulse-height spectrum expected from a BF_3 tube of very large dimension is exhibited (Knoll, 2000).

The spectral result obtained was similar to the spectral result produced in the manufacturer i.e. a quality certification. Based on the obtained results, the next stage was planned for the study of a proportional counter based on ^{3}He.

Basic preparation. We used a similar configuration for the proportional operation of the BP8 counter. The levels and polarities were configured for high voltage; specifically, the cathode was connected to a high negative voltage, the anode was isolated from the common point and the high voltage. Then the anode was connected to a new integrated circuit including a 149-86 signal amplifier. In this type of configuration a decoupled and isolated condenser for the high voltage in the output signal path is not required. One double resistor-capacitor network filter was connected between a high-voltage source and output to the cathode of a proportional counter to reduce the associated noise levels. These filters are similarly used to obtain a BP28 counter and show the same frequency cut-off response near 25 [Hz].

An LND25384 ^{3}He proportional counter with this configuration was connected with the high-voltage polarization of 1010 [V] recommended by the manufacturer. A multichannel analyzer was connected to a signal-pulse output, and the pulse-formation behavior was verified with the aid of a digital oscilloscope. These tests were performed over time periods of thirty minutes to several days. The obtained spectral amplitude was similar to that certified by the manufacturer.

The final design of the pulse amplifier-discriminator ^{3}He neutron counter builds on that of the amplifier used for the BF_3 neutron counter, taking into account the output voltage level of the ^{3}He neutron counter, which is below the level measured for the BF_3 neutron counter. The calibration of the initial stage of the charge-sensitive amplifier is performed experimentally by reducing the time-constant feedback loop and thereby increasing the level of primary gain to achieve sufficient amplification stage discrimination.

The full width at half-maximum (FWHM) of the neutron pulse distribution should be less than 20 [%] according to the IQSY manual to evaluate the possible deterioration of the BF_3 counter PB28. For the ^{3}He proportional counter, the calculated FWHM was 7.1% with the LND25384 and 8.7% with the LND25373.

The method used to verify the similar behaviors of the BP28-BF_3 and the ^{3}He LND25373 proportional counter

tubes consists of sequential steps. In the first step, we use the proportional counter BP 28, which is polarized, as a reference unit and verify its proper operation. This unit is then extracted and installed in a ^{3}He proportional counter for testing. The amplifier-discriminator was programmed to obtain the total amplitude spectrum from the minimum to the maximum high-voltage values applied to the proportional counter. Using the data obtained in the multi-channel analyzer, we calculated the FWHM values for each spectrum, beginning with the spectrum for 1200 [V], followed by sequential increases of approximately 28 [V] to a final a value of 1450 [V]. These spectra were normalized to 100% with respect to the channel with the maximum count; all channel values were referenced to this channel. The following test was conducted with the amplifier discriminator in the form of automatic gain control. We obtained a better spectrum shape and only a minor variance in the FWHM results at high voltage and low range.

The FWHM values are presented in Tables 1–3. The relation between pulse amplitude and applied voltage can generally be understood by considering the full width related to the half-maximum values or by the measurement of the spread of spectral distributions in the maximum sectors.

Fig. 1 presents the three most significant pulse-height distributions over the range of operating voltages for the ^{3}He LND25373 proportional neutron counter normalized with respect to amplitude and channel number. These results were obtained at high voltages of 1228 [V], 1312 [V], and 1338 [V] and selected from a spectrum at an operating voltage of 1200 to 1450 [V] with a moderator and aluminum support. The amplifier was set at a gain of 86149, the resistance was 37.33 [kOhm], and the gain control and discriminator level was 2.0.

The multichannel analyzer allows for the counting and classification of the output voltage pulse of the amplifiers connected to a proportional counter. Two types of spectra are classified: the coincidence and the anti-coincidence spectra. The coincidence spectrum is constructed only from pulses that trigger the discriminator circuit such that pulses below a threshold are rejected. The anti-coincidence spectrum is constructed without a previous discriminator circuit so that output pulses of all heights are utilized. The purpose of this step, using only the amplifier and the amplifier-discriminator, is to reject input pulses that are smaller than the limiting region given by the discriminator and allow for a comparison of their distribution so that the best value of the neutron counter bias can be determined.

2.4. Assembling the ^{3}He neutron monitor at the Los Cerrillos Observatory (OLC) for installation at LARC

As mentioned previously, the original geometry of the BF_3 neutron monitors was adopted in the assembly of ^{3}He neutron monitors. In the polyethylene reflector, a moderator and lead producer are also used although with a different diameter for the ^{3}He cylindrical counter: 5 [cm] versus BF_3: 14.5 [cm]. We designed and fabricated polyethylene end supports that maintain the original axial alignment of the counter and provide support for the cabinets that house the amplification and filtering systems for the high-voltage supply and act as a guide for the structure of the polyethylene moderator. The final assembly was sealed and operationally tested.

Fig. 2 shows the test spectrum obtained in the multichannel analyzer for the ^{3}He LND25373 neutron counter s/n 141695 and for the total anti-coincident spectrum counter detector in four possible experimental setups.

(a) With the bare counter, a total of 6892 [counts/hour] were produced.
(b) With only the polyethylene moderator and counter, a total of 8136 [counts/hour] were produced.
(c) With only the producer and counter, a total of 4877 [counts/hour] were produced.
(d) With the full setup including the moderator and the producer, a total of 27210 [counts/hour] were produced.

Such a ^{3}He neutron counter assembly with no moderator or producer, also called a neutron flux meter, was installed and made operational at the Antarctic Observatory LARC during the years 2007–2008 as a test of the long-term stability of the assembly and its response to extreme environmental conditions. The intensity-corrected average for

Table 1
Main characteristics and instruments of the Chilean Cosmic-Ray Observatories.

Station name	PUTRE	OLC	LARC	O'HIGGINS
Geographical	18° 11′ 47.8″ S	33° 29′ 42.3″ S	62° 12′ 9″ S	63° 19′ 15.6″ S
Coordinates	69° 33′ 10.9″ W	70° 42′ 59.81″ W	58° 57′ 42″ W	57° 54′ 0.36″ W
Station height [m] above sea level	3589	570	40	2
Geomagnetic latitude	8.17 S	23.40 S	52.32 S	53.42 S
Geomagnetic cutoff [GeV] (2010)	11.73	9.53	2.71	2.45
Instrumental setup				
Neutron monitor	3IGYNM-^{3}He	6NM64-BF_3	6NM64-BF_3 3NM64-^{3}He-CL 3NM64-^{3}He-IT	NM-^{3}He Facilities under study
Muon telescope	2-MMU	8-SMU	–	–
Magnetometer	UCLA-Fluxgate	UCLA-Fluxgate	UCLA-Fluxgate	UCLA-Fluxgate

Table 2
Proportional neutron counters for use in neutron monitors at the Chilean Cosmic-Ray Observatories.

Neutron counter	BP9-D	LND25384	BP-28	LND25373
Cathode material	Copper	Stainless steel	Stainless steel	Stainless steel
Maximum length [mm]	750	896.1	1908	1991.8
Maximum diameter [mm]	63.5	50.8	148.5	50.8
High-voltage operation [V]	2500	1000	2840	1300
High-voltage range [V]	2000–2900	900–1150	2600–3000	1200–1450
Resolution FWHM [%]	4.9	6	4.86	10
Gas filling	BF_3,^{10}B	^3He, CO_2	BF_3,^{10}B 96 %	^3He, CO_2
Gas pressure [Torr]	450	2280	200	3040
Gas filling volume [liters]	–	–	8.04	–
Active volume [liters]	2.3	1.65	33	3.86
Connector type	HN	HN	BNC-MHV	HN
Plateau slope [%/100 V]	2	$\leqslant 3$	1	$\leqslant 2$
Pulse height [mV]	1.5	1	1.5	1
Charge/pulse [Cb]	3.7E−13	1.0E−13	3.7E−13	1.0E−13

Table 3
Determination of FWHM at high voltage applied to a ^3He LND25373 proportional neutron counter.

High voltage operation	Test Ago02 FWHM [%]	Test Ago03 FWHM [%]	TestAgo04 FWHM [%]
1200	7.99	8.14	6.01
1228	6.47	6.96	5.94
1257	7.66	7.15	6.57
1285	7.95	8.75	6.95
1312	9.46	8.77	7.64
1338	8.76	10.18	8.62
1365	10.91	11.98	11.28
1393	12.61	10.48	13.11
1422	15.44	14.76	12.41
1450	13.28	14.74	14.01

September 2007 in the Antarctic Zone was approximately 8900 [counts/hour], as shown in Fig. 11; the standard deviation is approximately 1.30, whereas for the full ^3He neutron monitor, the standard deviation is approximately 0.6.

Our current interest is in the comparative study of environmental radiation at high latitudes, low latitudes and high altitudes. Only after these results are obtained can plans for the final ^3He counter design be drafted. Specifically, a preamplifier support structure unit that can deliver good protection and electrical shielding must be developed because these types of units are sensitive to surrounding electromagnetic changes.

The first test of both detector types involved the measurement of integral high pulses or amplitude spectra from discriminator systems. The LND25373 proportional counter was polarized at 1300 [V], and the amplifier-discrimination circuit was programmed for automatic gain-control operation. We registered the obtained data and made a parallel acquisition platform with the acquisition data systems of the Multidirectional Muon Telescope and the 6NM64 neutron monitor under continuous operation. In this configuration, we compared the results with the temporal variation of these instruments. In addition, we compared the data obtained for the ^3He and BP28 proportional neutron counters and performed a simultaneous multichannel analyzer test, with a minimum duration of 24 [h].

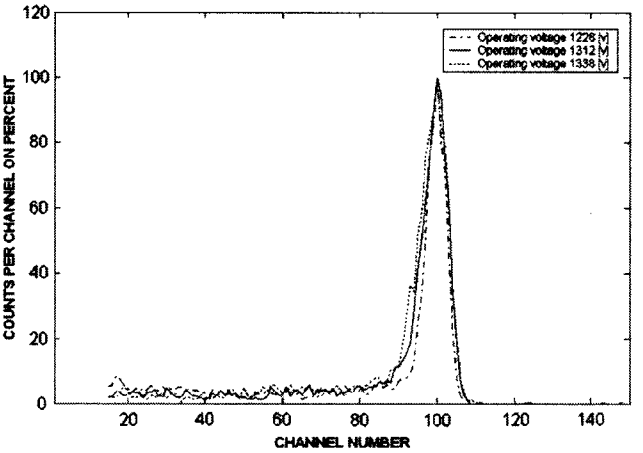

Fig. 1. Multichannel pulse height distribution for an LND25373 ^3He neutron counter. This tests are been normalized by amplitude and maximum channel number.

The first group of tests ultimately determined the activity of the output pulses of the proportional counter, which remained polarized at a high voltage. In the Ago20 test, the discriminator level was modified to a maximum level in the LND25373 counter, allowing for many tests with temporal variations over a long period of time. A better relationship with the temporal data for the same period was obtained with the IQSY 6*NM*64 neutron monitor. These data represent the uncorrected daily variations of the BP28 counters.

3. Results

3.1. The response of the ^3He neutron monitor in the detection of secondary cosmic rays arriving at the stations after three years of continuous operation

At the OLC and the LARC in Antarctica, we began simultaneous cosmic-ray registration with the 6NM64 and ^3He neutron monitors with the same type of high-voltage supply set at level of 2840 [V] and 1300 [V], respectively, and recorded the atmospheric pressure over the same period of data acquisition.

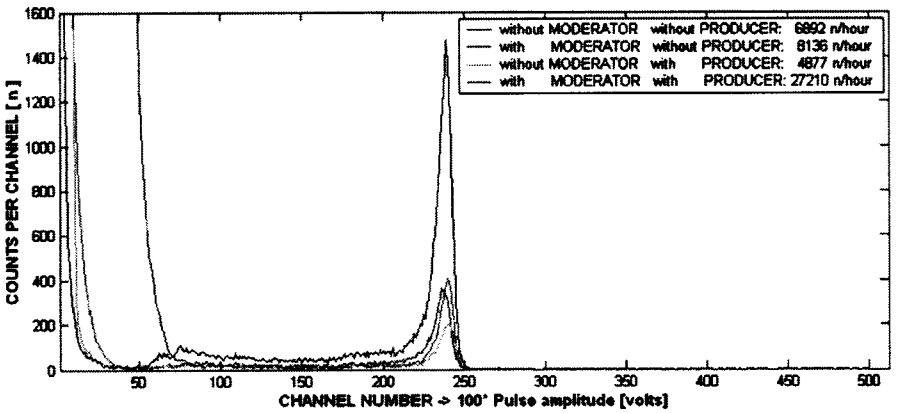

Fig. 2. Multichannel test of the ^{3}He LND25373 proportional neutron counter. The time for each test was one hour. The results of four tests are shown, each test with a different configuration of the moderator and producer envelope.

At the Putre-Incas High-Mountain Cosmic-Ray Observatory, which features an IGY ^{3}He neutron monitor, the level was set to 1100 [V]. Fig. 3 presents one obtained pulse amplitude spectrum.

3.2. The calculation of the Putre-Incas High-Mountain 3IGYNM-^{3}He barometric coefficient

The original data files for each station are stored in real time in a database in Santiago (OLC). This database contains data regarding date, Julian date, universal time coordinates, recording time, atmospheric pressure at the station (mm Hg or hPa), 5- or 1-min counting rates registered by each proportional counter or in sections of BF_3 or ^{3}He, relative humidity and temperature.

One preliminary data treatment features data-string decoding, data-format check with data recovery if possible when a failure is present, station pressure check, file setup, monitor stability check by means of the proportional counter section ratios, hourly averages of registered cosmic-ray intensity and the station atmospheric pressure file setup.

After this preliminary data treatment, as a first operational test, we calculated the estimated attenuation coefficients or barometric coefficients of each station on daily, monthly and yearly bases using different techniques to obtain the intensity data of the cosmic rays corrected for pressure variations.

The barometric modulation shown in Fig. 4 in the neutron monitor counts caused by atmospheric pressure changes can be large; this treatment must be carefully executed, with the objective of revealing the primary variations in the counting rates of the detectors. The temperature effects are usually small and can thus be neglected.

In this process, we compare the results obtained with three statistical methods: standard or simple regression (S), a difference filter (D) and an autoregressive filter (A).

The database used contains the 3IGYNM-^{3}He neutron monitor data recorded in September 2007 at the Putre-Incas High-Mountain Observatory.

Number of data records: 3063, (covering approximately 128 days)

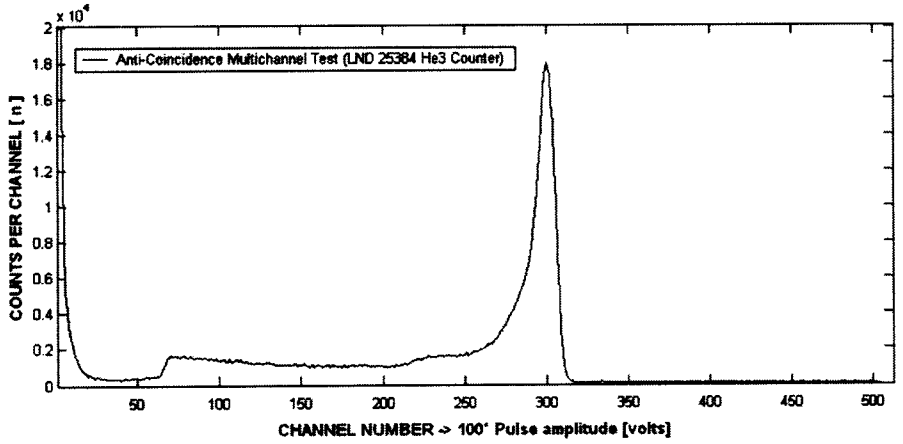

Fig. 3. Pulse amplitude distribution obtained for the LND25384 ^{3}He neutron counter operating in the 3IGYNM-^{3}He neutron monitor at the Putre-Incas High-Mountain Cosmic-Ray Observatory.

S: Standard or simple regression method
A: Autoregressive filter method
D: Difference filter method
NDS: Number of data segments (1 to 4; 5 in total)
Ndata: Number of data records
Beta: Barometric coefficient
Error: Coefficient error
Cor: Coefficient of correlation between pressure and intensity
Cacr: Coefficient of auto-correlation of the residues
Sr2: Sum of the squared residues
Average segment pressure
Average segment intensity
The values calculated for each segment were applied to all pressure-intensity pairs to estimate the final barometric coefficients.

S Beta: 0.8253 Err: 0.0149
A Beta: 0.8189 Err: 0.0266
D Beta: 0.8438 Err: 0.0476

3.3. The atmospheric response and yield function

The ground-based neutron monitor is a primary cosmic-ray detector. The world's neutron monitor network is a state-of-the-art instrument used to measure primary cosmic-ray variations in the rigidity range of 1 to 15 [GeV]. With stations at effective cutoff rigidities of 11.74, 9.53 and 2.71 [GeV] (IGRF 2010), the Chilean cosmic-ray neutron monitors constitute an important component of the existing network.

In general, our work was experimental; thus, it is important that the detection responses of these neutron monitors to secondary cosmic-ray particles are known. We present a brief summary of the modeling and numerical simulation applied to the 3IGYNM-^{3}He Putre data using the Geant4 Monte Carlo code (Agostinelli et al., 2003) to survey the response of the high-mountain neutron monitor to the total flux that arrived in an atmospheric shower of primary cosmic rays.

Moreover, the neutron monitor data are used to determine the characteristics of solar and galactic cosmic-ray fluxes in the Earth for which we must evaluate atmospheric particle transport and neutron monitoring efficiency. To this end, we must account for the yield function S using the counting rate N for epoch t according to the classical expression (Clem, 1999; Clem and Dorman, 2000)

$$N(Pc,z,t) = \int_{Pc}^{\infty} \sum_i S_i(P,z) \cdot Ji(P,t)\, dP = \int_{Pc}^{\infty} W_T(P,z,t)\, dP \quad (1)$$

$$S_i(P,z) = \sum_j \iint Aj(E,\theta) \cdot \Phi_{ij}(P,z,E,\theta)\, dE\, d\Omega \quad (2)$$

where $N(P,z,t)$ is the neutron monitor counting rate, P is the primary particle rigidity, i is the primary particle (proton or alpha), Pc is the geomagnetic cutoff, z is the atmospheric depth, t is the epoch, $S_i(P,z)$ represents the yield function for the primary rays of particle type i, J_j (P,t) represents the primary particle rigidity spectrum type i at epoch t, A_j is the effective area, Φ_{ij} is the differential flux

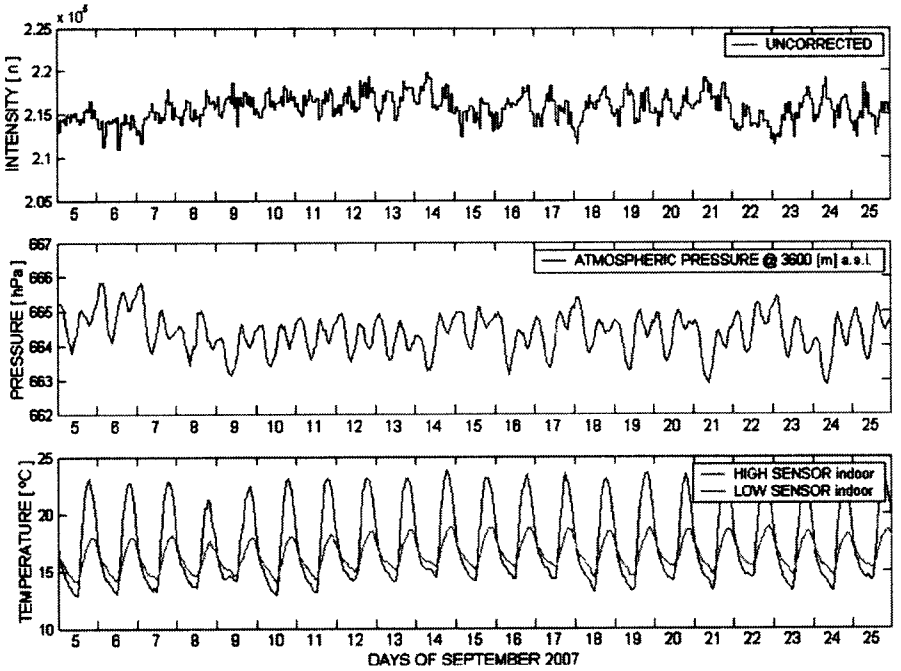

Fig. 4. 3IGYNM-^{3}He neutron monitor total uncorrected count, atmospheric pressure and indoor temperature measured at the Putre-Incas High-Mountain Cosmic-Ray Observatory, September 2007.

of secondary particles per primary, E is the secondary particle energy, θ and Ω are the secondary particle angle of incidence and the solid angle, respectively, and W_T is the total differential response function.

The yield function shown corresponds to the 3IGY-NM-^{3}He neutron monitor installed at the Andes Mountain Range Altiplane in the town of Putre using the local rigidity cutoff and atmospheric depth as parameters. The yield function is evaluated as the sum of the convolution between the detector's efficiency and the differential atmospheric neutron and proton flux per primary particle.

We used the Geant4 Monte Carlo code to determine the efficiency of the 3IGYNM-^{3}He monitor for detecting incident secondary particles. The monitor geometry and constituent materials are listed in detail in Section 2.2. The simulation consists of an evaluation of the monitor response to a parallel beam of particles with different energies directed from the zenith over the detector, specifically for neutrons and protons.

In Figs. 5 and 6, we illustrate the effective area obtained from the simulation of the 3IGYNM-^{3}He monitors for vertically falling neutrons and protons. The effective area was calculated by employing the geometric area of the monitor's upper surface, and the efficiency was calculated as the relation (Nc/Ni) between the number of neutrons and protons captured in the counters and the number of incident atmospheric neutrons and protons. The efficiency responses for the new ^{3}He counters and the older BF_3 counters they replaced are shown. These results are in agreement with the empirical variation quotient of 10% obtained at the LARC Antarctic Observatory.

The degree of particle transport through the atmosphere was obtained via the secondary neutron and proton spectrum generated by the primary particles, with isotropic

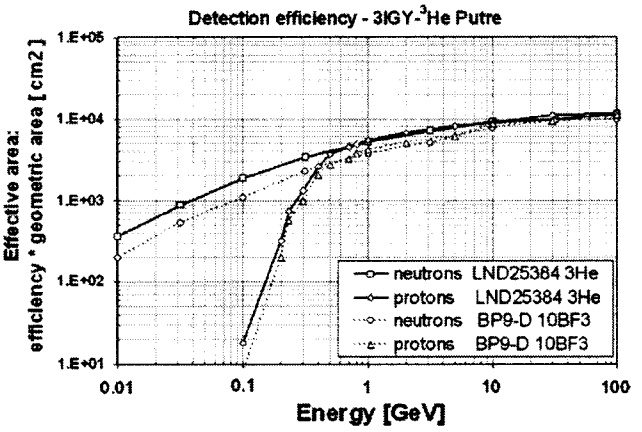

Fig. 6. Effective area of the 3IGYNM-^{3}He detector for neutrons and protons with vertical incidence. The energy scale is for secondary particles. The responses of the ^{3}He and BF_3 detectors are compared.

incidence at the top of the layers; these values were calculated for atmospheric depths between 600 and 1033 [g/cm^2] and primary energies between 0.01 and 20 [GeV], which is within the range of the geomagnetic rigidity cutoff. The simulation of this process was performed using the Geant4 Planetocosmics code (Atmocosmics code, 2004; Desorgher et al., 2005; Desorgher, 2006).

The 3IGYNM-^{3}He monitor yield function for primary protons is presented in Fig. 7; this function was obtained from the differential flux spectra for secondary particles, neutrons and protons generated by the energy of the primary protons during the minimum solar activity period. The corresponding values at the entrance to the neutron monitor were calculated from the monitor's efficiency function with respect to secondary particles. The energy scale shown ranges from 1 to 18 [GeV].

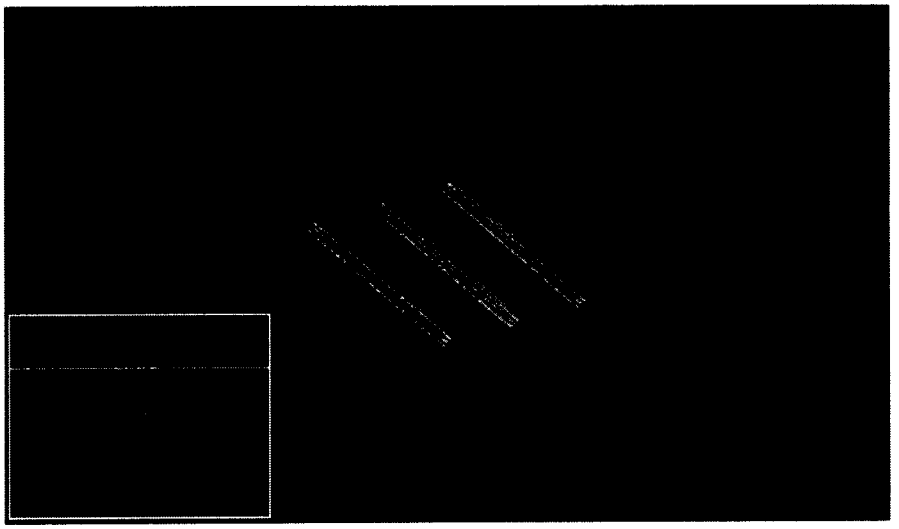

Fig. 5. Example of monitor geometry interacting with incident particles; one simple step of the simulation is shown. The green lines are the neutron paths, and the yellow shapes are the ^{3}He counters. The details show one neutron capture in the ^{3}He gas detector; the blue paths are the trajectories of the reaction products: positively charged protons and tritons. (For interpretation of the references to colour in this figure legend, the reader is referred to the web version of this article.)

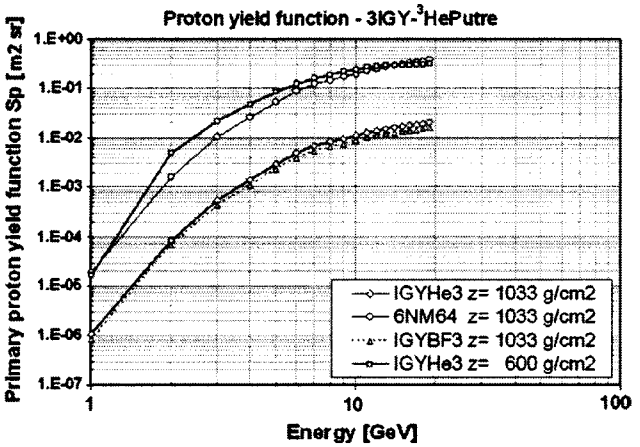

Fig. 7. Proton primary yield function for the 3IGYNM-^{3}He neutron monitor. The results are compared with those using the ^{3}He and BF_3 neutron counters for two atmospheric depths. The 6NM64 neutron monitor response is shown as a reference.

The proton yield function for the 6NM64 monitor at 1033 [hPa] was calculated using the traditional Monte Carlo computation as described by Clem and Dorman (2000) and Flückiger et al. (2008). In the same manner, we obtained the values of the proton yield function for the 3IGYNM-^{3}He monitor at 1033 [hPa] and at 600 [hPa] and the IGYNM-BF_3 monitor at 1033 [hPa] and at 600 [hPa]. The BP9-D BF_3 counters were then replaced with the LND25384 ^{3}He counters.

The yield function calculated for the Putre high-mountain monitor is similar to the results obtained with the IGY configuration for other latitudes and stations. The shape and values for this monitor are compared with those of the 6NM64 monitor parameterized by Flückiger et al. (2008).

The total differential yield functions of the primary particles during the solar minimum are shown in Fig. 8 for

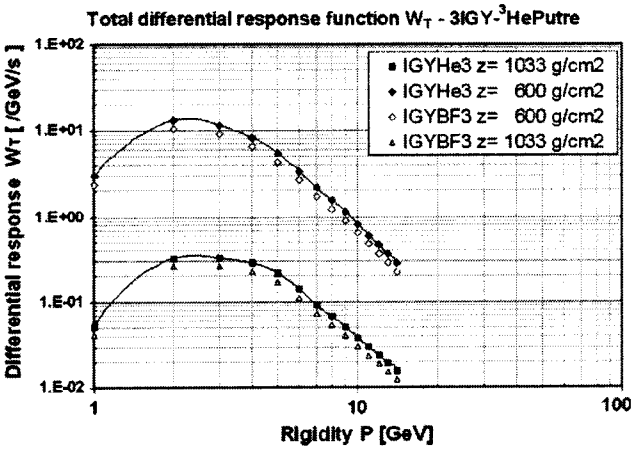

Fig. 8. The differential total response function of the Putre 3IGYNM-^{3}He neutron monitor at sea level and at high-mountain elevation. The comparative responses using the ^{3}He and BF_3 neutron counters are also shown.

atmospheric altitudes ranging from sea-level to high-mountain elevations; the functions are compared with the changes in the BF_3 counters and ^{3}He counters and also the differential response functions of the 3IGYNM-^{3}H neutron monitor for high-mountain and sea-level elevations, for which the atmospheric depth is easily comparable. These results are shown in Fig. 7 along with the results of several previous studies using Monte Carlo simulations or parametric methods (Dorman and Yanke, 1981; Lockwood et al., 1974; Moraal et al., 1989; Nagashima et al., 1989; Stoker, 1981).

4. Discussion

The original goal of this study was to determine the possibility of replacing the old proportional tubes of the BF_3 monitor with the ^{3}He proportional counter in standard IQSY neutron monitors and IGY neutron monitors for use in our observatories. This would allow for new neutron monitoring detectors that could be used for the next ten or twenty years with better confidence and efficient, long-term operation without failure to improve the range of detection for particles arriving as galactic and solar cosmic rays. In understanding the fundamental characteristics of the new instrument, the main issue in recent years has been determining how to implement these characteristics in the 6NM64-BF_3 monitor (Cordaro, 1991; Cordaro and Storini, 1992a,b; Cordaro et al., 1992; Storini and Cordaro, 1997).

We calculated the FWHM values in steps of 28 [V] over a spectrum ranging from 1200 [V] to 1450 [V]. The best values obtained for the FWHM were 6.01%, 5.94%, 6.57%, 6.95% and 7.64% at 1200, 1228, 1257, 1285 and 1312 [V], respectively, which corresponds to the high-voltage range [volts] of the LND25373 ^{3}He proportional counter. The same test was performed to determine the activity of the output pulses of the proportional counter, calculate the FWHM and obtain, under the same technical conditions applied to the ^{3}He LND25373 monitor, the amplitude distribution obtained for the LND25384 at a high-mountain observatory.

We eliminated the pressure dependence of the counting rate and determined the primary cosmic variations at all observatories. At the OLC, the calculated attenuation coefficient for the year 2007 and the BF_3 neutron counter was (0.672 ± 0.011) [%/hPa], with an average pressure level of 955 [hPa]. At the LARC, the calculated attenuation coefficient for the year 2007 was (0.740 ± 0.012) [%/hPa] for the BF_3 neutron counter and (0.739 ± 0.009) [%/hPa] for the ^{3}He neutron counter, with an average pressure level of 980 [hPa]. At Putre-Incas, the value was (0.8253± 0.0014) [%/hPa], with an average pressure level of 666 [hPa] (Cordaro and Storini, 1995; Cordaro and Storini, 2001).

The increased intensity justifies the change in the type detector used due to the better resolution afforded. For example, at the Antarctic Observatory LARC, the average intensity [counts/counter] obtained for the 3NM64-^{3}He

neutron monitor is 10% larger than the average intensity [counts/counter] obtained for the 6NM64-BF_3 neutron monitor, as shown in Fig. 9. Moreover, the simulation performed with the Monte Carlo method using the Geant4 code reveals a better detection efficiency using the ^{3}He neutron counter. The numerical results obtained are in agreement with a rate increase of 33.5 [%], using the integration of the W_T function for the BF_3 and ^{3}He neutron counter.

Fig. 10 illustrates the intensity recorded with the BF_3 proportional counter, where we have eliminated the dependence of the counting rate on the pressure level at each station in the Cosmic-Ray Observatory network in the Oriental sector of the Pacific Ocean or the Andes Mountain range in the southern hemisphere.

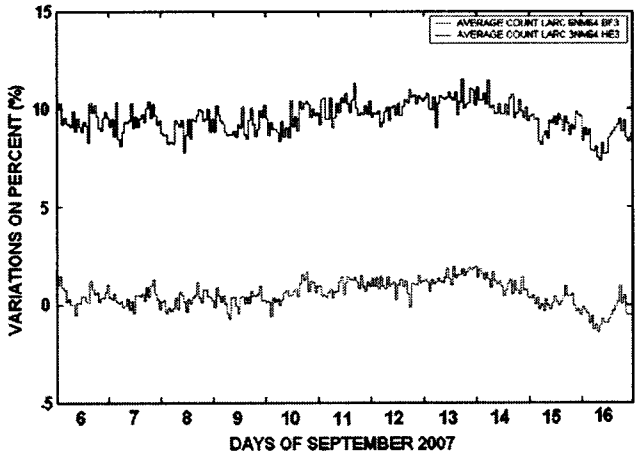

Fig. 9. The average counts for the ^{3}He neutron counter versus the average counts for the BF_3 neutron counter, showing an increase of more than 10%.

This example includes the cosmic-ray event occurring in December 2006. The variations between the amplitude of the intensity recorded in the Forbush Decrease are well reproduced at each station. The decrease at Putre-Incas is approximately 4%, that at Los Cerrillos is approximately 6% and that at the Antarctic-LARC is approximately 9%. These values are related to the cutoff geomagnetic rigidity at each station. On December 13th, the intensity peak corresponding to the Ground-Level Event beginning at time 0300 [UTC], generally caused by the arrival of flow-energy solar protons in the polar cap absorption, was not detected at the low-latitude stations. On December 13th and December 14th, we generally observed Type IV radio emissions and a Geomagnetic K index ranging from 4 to 7, with a maximum peak at 7. Several authors have noted the existence of a decrease in cosmic rays preceding the front of the shock wave of the interplanetary magnetic field collimated outward flow across the shock from the inside of the Forbush Decrease (Nagashima et al., 1992; Nagashima et al., 1993). This is typically observed using muon detectors (Fusishita et al., 2010).

In our case, the detectors are neutron monitors around the Oriental sector of the Pacific Ocean or the Andes Mountain range in the southern hemisphere. The characteristics of the events of December 2006 are similar with respect to the sudden commencement (SC) of the geomagnetic storm. Prior to the occurrence the Forbush Decrease, a clear concavity appeared for ten hours in the cosmic-ray intensities; these were associated with the initial decrease caused by the IMF linkage with low-density cosmic rays

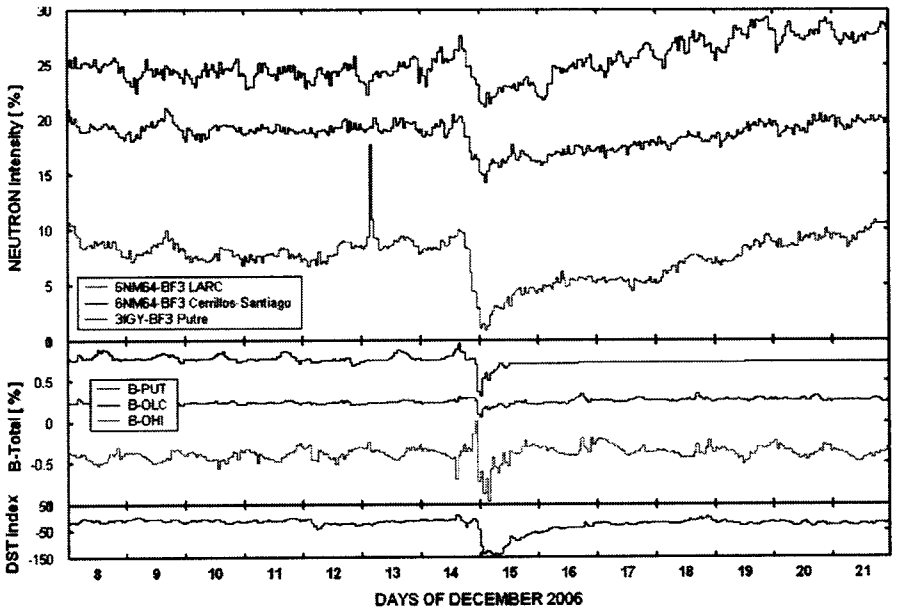

Fig. 10. The hourly neutron counting rates corrected for pressure, the possible precursors of the Forbush Decrease, the ground level event Number 70 and the Forbush Decrease of December 2006 at the Cosmic-Ray Observatories in the southern hemisphere sector of the Oriental Pacific Ocean from low to high latitude. The geomagnetic B-total field and the DST index are shown.

Table 4
Calculated barometric coefficients for the Putre-Incas High-Mountain Cosmic-Ray Observatory 3IGYNM-^{3}He neutron monitor data for September 2007.

	N D S	Ndata	Barometric coefficient beta	Error	Cor	Cacr	Sr^2	Average pressure	Average intensity
S	1	612	0.7486	0.0343	−0.6618	0.6671	0.0252	664.38	215204
A	1	612	0.7514	0.0624	−0.4385	0.2178	0.0140	664.38	215204
D	1	612	0.7558	0.0953	−0.3056	−0.4398	0.0168	664.38	215204
S	2	612	0.9367	0.0261	−0.8235	0.6494	0.0213	664.27	216185
A	2	612	0.9222	0.0489	−0.6072	−0.1779	0.0123	664.27	216185
D	2	612	0.8918	0.0860	−0.3869	−0.4050	0.0148	664.27	216185
S	3	612	0.9189	0.0310	−0.7687	0.6182	0.0211	663.59	217602
A	3	612	0.9155	0.0553	−0.5567	−0.1975	0.0130	663.59	217602
D	3	612	0.8976	0.0975	−0.3492	−0.4491	0.0161	663.59	217602
S	4	612	0.6567	0.0293	−0.6714	0.5352	0.0198	663.76	217280
A	4	612	0.6803	0.0491	−0.4891	−0.1308	0.0142	663.76	217280
D	4	612	0.8167	0.1046	−0.3013	−0.4237	0.0184	666.76	217280
S	5	614	0.8181	0.0322	−0.7161	0.5188	0.0163	663.83	218114
A	5	614	0.8332	0.0513	−0.5488	−0.1332	0.0119	663.38	218114
D	5	614	0.8829	0.0959	−0.3489	−0.4410	0.0156	663.38	218114

Table 5
Initial intensity levels and geomagnetic records at the Chilean Cosmic-Ray Observatory stations in September 2007.

Station name	PUTRE INCAS	SANTIAGO OLC	ANTARCTICA LARC	ANTARCTICA O'HIGGINS
Initial level on September 1, 2007, [00 h]				
Neutron monitor total [counts/hour]	3IGYNM-^{3}He 215036	6NM64-BF_3 237676	6NM64-BF_3 279246 3NM64-^{3}He 152637 NM Bare ^{3}He 9086	NM-^{3}He Facilities under study
Muon telescope vertical [counts/hour]	2-MMU 121869	8-SMU 283010	–	
Magnetometer total: B [nT]	22326	24628	43944	38158

across the magnetic shock inside the Forbush Decrease collimated with the IMF. The increase in the neutron rate is related to the pitch angle, and the IMF and reflects an interplanetary shock with an estimated velocity of approximately 1277 [km/s] (Space Weather Alerts et al., 2006).

Apparently, similar events developed at the Putre-Incas High-Mountain Observatory near the equatorial zone and the LARC Antarctic Observatory: a clear decrease in the level observed at each station ten hours prior to the SC. Despite their different geographic locations and geomagnetic cutoff rigidities, the great change in the total magnetic field registered in both magnetic sensors during the period of Forbush Decrease. The geomagnetic wave possesses a minor amplitude at high latitude. This is only a first observation of the events of December 2006 due the shock-reflected particles measured by the cosmic-ray observatory network around the Oriental sector of the Pacific Ocean or the Andes Mountain range.

These results must reflect the technical conditions of each stage of the design and construction of the different parts of the new ^{3}He cosmic-ray neutron monitors at Putre Incas and the entire network of observatories around the Oriental sector of the Pacific Ocean and the Andes. The theoretical data from all network observatories were treated, and we present the calculations made for the Putre measurements except for small and insignificant differences at each place, which we neglect.

The original data files for each observatory are stored in a database at the Santiago OLC. The record types and data treatment are presented in Fig. 4 for the 3IGYNM-^{3}He neutron monitor, with a total uncorrected count of approximately 215,000 [counts/hour] and an average atmospheric pressure of 666 [hPa] at room temperature. The average high and low temperatures measured at the Putre-Incas High-Mountain Cosmic-Ray Observatory in September 2007 were approximately 19 [°C] and 17 [°C], respectively.

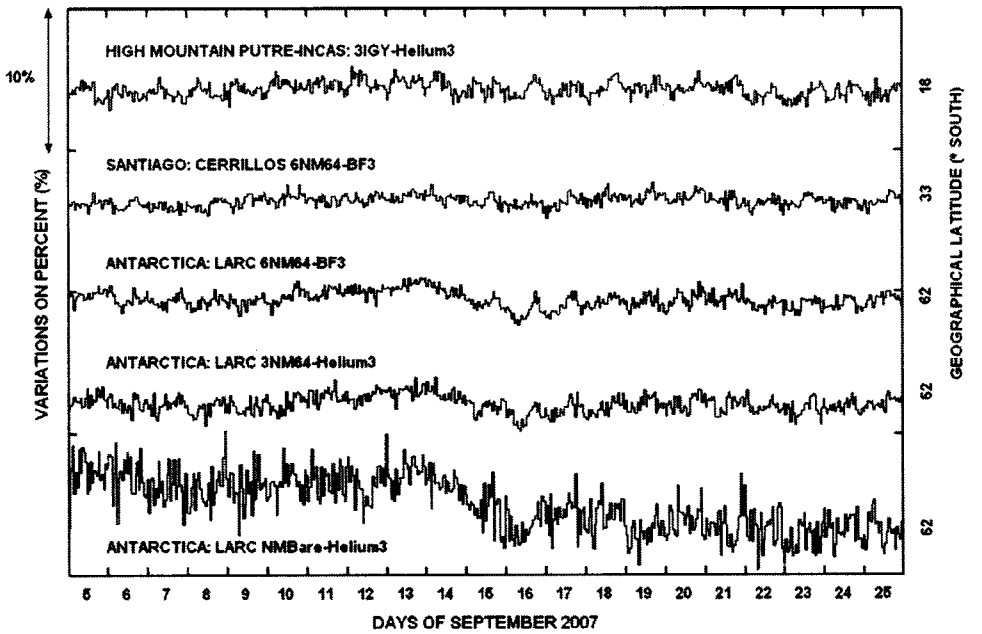

Fig. 11. Time history of nucleonic intensities at the Chilean Cosmic-Ray Observatories for September 2007. The operation of the ^{3}He neutron counter is shown along with the operation of the BF_3 neutron counter.

We calculated the estimated attenuation coefficients using several different techniques. In this calculation, the barometric modulation in the neutron monitor counts due to atmospheric pressure changes could be large, so this treatment must be carefully executed with the objective of revealing the primary variation in the counting rate of the detectors.

Tables 4 and 5 summarizes the initial intensity and geomagnetism levels for the detectors used in the network during a quiet period in September 2007.

The operation of the ^{3}He neutron counter together with the operation of the BF_3 neutron counter for the entire network of Cosmic-Ray Observatories is illustrated in Fig. 11; the shapes of the cosmic-ray intensities are similar yet differ in amplitude due to the rigidity cutoff. The geomagnetic cutoff for the Putre-Incas Observatory is 11.73 [GeV], that of the OLC is 9.53 [GeV] and that of the LARC is 2.7 [GeV]. We have presented many instrumental and theoretical tests for long-term research in remote places that are difficult to access in Antarctica and the Andes, which are locations with long periods of isolation and harsh ambient conditions (Villalon-Rojas, 2009).

5. Conclusions

We tested the LND25373 and LND25384 counters in the standard configuration for neutron monitors equipped with BP-28 counters and the traditional 3IGYNM neutron monitors equipped with BP9-D counters. These tests were conducted at two sites: the Antarctic and Altiplanic zones in the Andes Mountains and the Oriental South Pacific Ocean in the southern hemisphere.

The responses of both types counters are similar with respect to atmospheric variations, yielding enhancements of approximately 3–3.5% at low latitudes and to 9–10% for high latitudes, where the ^{3}He counter was used for primary cosmic-ray variation. The counting rate of the ^{3}He counter was consistently higher than the rates of the BP-28 and BP9-D counters.

The testing of the amplifier and discriminator system for both types of ^{3}He counters (Ago02, Ago03,...) was performed with the amplifier discriminator in fixed-gain mode. The next test (Ago09) was performed with automatic gain control for the amplifier discriminator. We obtained a better spectrum shape with only a minor variation in the FWHM results over the entire voltage range investigated. To determine the effects of the detectors physical dimensions and electrical characteristics, the BP28 counters in NM64 neutron monitors were replaced with LND25373 units, and the BP9D counters in the IGY neutron monitors were replaced with LND25384. We compared the results obtained in 2007 at the Putre-Incas observatory in the Andes Mountains by treating the daily data from the 3IGYNM-^{3}He neutron monitor with three statistical methods: standard or simple regression (S), a difference filter (D) and an autoregressive filter (A).

In this work, we evaluated the detection efficiency, yield function and total differential response of the 3IGY-NM-^{3}He detector by means of Monte Carlo simulations, with a treatment of the particle interaction and atmospheric cascade using the Geant4 toolkit. The results are in agreement with those for similar IGY configurations, and in this case, the simulation was computed for this specific neutron monitor for the first time. Sections 2–4 of this

paper present details regarding the instrumental calibrations that are fundamental to monitor operation, which were obtained through many experimental studies during station operations (from 1960 to 2011). In recent years, the simulation process described in Section 3.3 has helped to complement and improve neutron monitoring detector efficiency. Only after an extended testing process will we replace the older BF_3 counter with the new ^3He counter.

The data collected using the neutron monitors and the barometric data collected at the stations over a long time period reflect the technical conditions experienced during each stage of the design and construction of the different parts of the new monitor. We compared the results from the BF_3 neutron monitors in the stations in Santiago, Chile, the BF_3 and ^3He neutron monitors in Antarctica and the IGY ^3He neutron monitor at Putre-Incas, in the Andes. An interesting aspect of this collaboration for cosmic-ray research has been the sharing of the experiences and experimental results obtained through this process with the scientific community; these results may be useful in planning for the installation of new neutron monitors.

More than three years of research assessing neutron-counter performance and the ambient conditions of the Putre-Incas (Altiplanic Zone), OLC in Santiago (Meridional Zone) and Antarctic (Antarctic Zone) observatories ensure the collection of high-quality data for the study of solar-terrestrial relations in near-equatorial to Antarctic zones in sectors of the South Oriental Pacific Ocean and the Andes Mountains in the southern hemisphere.

Acknowledgements

The authors thank Dr. M. Storini (IFSI-Roma), Dr. M. Parisi (UNI-Roma Tre) and Dr. E. Zesta (UCLA-IGPP) for their collaborations and advice. Dr. L.A. Raggi (Incas-UCh) for their collaboration and support. The neutron monitors at the LARC, OLC and Putre-Incas Observatories are partially supported by FCFM-University of Chile, with antarctic logistical support from INACH. Partial instrumental support is also provided by IFSI-Roma, UNI-Roma Tre and PNRA of Italy. We also wish to thank the following groups: the Antarctic Division of the Chilean Air Force and the E. Frei Base King George Island; the airport gateway to the Antarctic territory for their continuous collaborations and aid; the Antarctic Department of the Chilean Army and the Gen. B. O'Higgins Base on the Antarctic Peninsula for their continuous collaborations and aid; and the UCLA-IGPP fluxgate magnetometer, in collaboration with the South American Magnetometer B-field Array (SAMBA) project of the University of California, Los Angeles, USA. Also, we would like to thank to the anonymous Referees for their comments and suggestions. D.L. acknowledges partial financial support from Fondecyt 11080229 and Fondecyt 1120764, the Millennium Scientific Initiative, $P10-061-F$, the Basal Program Center for the Development of Nanoscience and Nanotechnology (CEDENNA) and Performance Agreement Project UTA/ Mineduc UTA-Project 8750-12. D.S.A acknowledges CONICYT PhD program fellowship.

References

Agostinelli, S., Allisonas, J., Amako, K., et al. Geant4-a simulation toolkit. Nucl. Instrum. Methods Phys. Res. A 506, 250–303, 2003.

Atmocosmics code, Version 1.0, <http://reat.space.qinetiq.com/septimess/atmcos/>, 2004.

Clem, J.M., Atmospheric yield functions and the response to secondary particles of neutron monitors, in: Proceedings of the 26th International Cosmic Ray Conference, 1999, Salt Lake City, USA, vol. 7, pp. 317–320, 1999.

Clem, J.M., Dorman, L.I. Neutron monitor response functions. Space Sci. Rev. 93, 335–359, 2000.

Cordaro, E.G., Progress in the Chilean Cosmic Ray Laboratories, in: Proceedings of the 26th International Cosmic Ray Conference, 199, Dublin, Ireland, vol. 3, pp. 800–803, 1991.

Cordaro, E.G., Storini, M. The response of Los Cerrillos detectors to 1989/1990 G.L.E. events. Geofisica Internacional 31 (1), 65–78, 1992a.

Cordaro, E.G., Storini, M. Cosmic Ray Measurements in Antarctica during the International Solar-Terrestrial Energy Program. Nuovo Cimento C 15 (5), 539–545, 1992b.

Cordaro, E.G., Johnson, E.R., Storini, M. A neutron monitor on King George Island. Geofisica Internacional 31 (1), 79–87, 1992.

Cordaro, E.G., Storini, M. LARC/6-NM-64 Atmospheric pressure effects. Serie Cientifica del Instituto Antartico Chileno 45, 67–88, 1995.

Cordaro, E.G., Storini, M. On the use of the South-American neutron monitors. Nuovo Cimento C 24 (4-5), 683–689, 2001.

Desorgher, L., Flückiger, E.O., Gurtner, M., et al. Atmocosmics: A Geant4 code for computing the interaction of cosmic rays with the Earth's atmosphere. Int. J. Modern Phys. A 20 (29), 6802–6804, 2005.

Desorgher, L. The PLANETOCOSMICS code, Version 2.0, <http://cosray.unibe.ch/-laurent/planetocosmics>, 2006.

Dorman, L., Yanke, V. The Coupling Functions of the NM-64 Neutron Supermonitor, in: Proceedings of the 17th International Cosmic Ray Conference, 1981, Paris, France, vol. 4, p. 326, 1981.

Flückiger, E.O., Moser, M.R., Pirard, B., et al. A parameterized neutron monitor yield function for space weather applications, in: Proceedings of the 30th International Cosmic Ray Conference, 2007, Merida, Mexico, vol. 1, pp. 289–292, 2008.

Fusishita, A., Kuwabara, T., Kato, C., et al. Precursors of The Forbush Decrease on 2006 December 14 Observed with the Global 2Muon Detector Network (GMDN). Astrophys. J. 715 (2), 1239, 2010.

Knoll, G.F. Radiation Detection and Measurement, third ed John Wiley & Sons, New York, USA, 2000.

Lockwood, J.A., Webber, W.R., Hsieh, L. Solar flare proton rigidity spectra deduced from cosmic ray neutron monitor observations. J. Geophys. Res. 79, 4149–4155, 1974.

Mills Jr., W.R., Cadwell, R.I., Morgan, I.L. Low voltage He3 filled proportional counter for efficient detection of thermal and epithermal neutrons. Rev. Sci. Instrum. 33 (8), 866–868, 1962.

Moraal, H., Potgieter, M.S., Stoker, P.H., van der Walt, A.J. Neutron monitor latitude survey of cosmic ray intensity during the 1986/1987 solar minimum. J. Geophys. Res. 94, 1459–1464, 1989.

Nagashima, K., Sakakibara, S., Murakami, K., Morishita, I. Response and yield functions of neutron monitor, galactic cosmic ray spectrum and its solar modulation, derived from all the available world-wide surveys. Nuovo Cimento C 12, 173–209, 1989.

Nagashima, K., Fujimoto, K., Sakakibara, S., Morishita, I. Local-time-dependence pre-IMF.shock decrease and post-shock increase of cosmic ray, produced respectively by their IMF-collimated outward and inward flows across the shock responsible for Forbush Decrease. Planet. Space Sci. 40, 1109–1137, 1992.

Nagashima, K., Sakakiraba, S., Fujimoto, K. Local-time-dependent pre-IMF-shock decrease of cosmic rays, produced by their IMF-collimated outward flow across the shock from the inside of forbush decrease. J. Geomagnetic Geoelectr. 45, 540–553, 1993.

Simpson, J.A., Fonger, W.H., Treiman, S.B. Cosmic radiation intensity-time variations and their origin, I, Neutron intensity variation method and meteorological factors. Phys. Rev 90, 934, 1953.

Space Weather Alerts, Alerts Time line Archive for December 1–15, 16–31, http://www.swpc.noaa.gov/alerts/archive/archive_01Dec2006.html, 2006.

Stoker, P.H. Primary spectral variations of cosmic rays above 1 GV, in: Proceedings of the 17th International Cosmic Ray Conference, 1981, Paris, France, vol. 3, pp. 193–196, 1981.

Storini, M., Cordaro, E.G. Italia/Chile Colaboration for LARC. IL Nuovo Cimento C 20, 1027–1032, 1997.

Vekler, V., Groshev, L., Isayer, B. Ionizations methods for studying radiations Gostekhizat, 1950.

Villalon-Rojas, E. 2do Memorial Antártico del Ejército, Ejercito de Chile, Punta Arenas Chile, 2009.